Papers

Quality assessment of atmospheric surface fields over the Baltic Sea from an ensemble of regional climate model simulations with respect to ocean dynamics*

OCEANOLOGIA, 53 (1-TI), 2011.
pp. 193–227.

KEYWORDS
Regional climate modelling
Atmosphere-ocean coupling
Climate change
Ensemble modelling
Baltic Sea region

H. E. Markus Meier[1,2,⋆]
Anders Höglund[1]
Ralf Döscher[1]
Helén Andersson[1]
Ulrike Löptien[1]
Erik Kjellström[1]

[1] Swedish Meteorological and Hydrological Institute,
Research Department,
Norrköping 60176, Sweden

[2] Department of Meteorology,
Stockholm University,
Stockholm 10691, Sweden;

e-mail: markus.meier@smhi.se

⋆corresponding author

Received 6 October 2010, revised 27 January 2011, accepted 28 January 2011.

* The work presented in this study was jointly funded by the Swedish Environmental Protection Agency (SEPA), the Swedish Research Council for Environment, Agricultural Sciences and Spatial Planning (FORMAS), and the European Commission within the projects ECOSUPPORT (Advanced modelling tool for scenarios of the Baltic Sea ECOsystem to SUPPORT decision making, ref. no. 08/381), AMBER (Assessment and Modelling Baltic Ecosystem Response, ref. no. 08/390) and INFLOW (Holocene saline water inflow changes into the Baltic Sea, ecosystem responses and future scenarios, ref. no. 2008–1885). All three projects are part of the BONUS+ program (http://www.bonusportal.org).

Abstract

Climate model results for the Baltic Sea region from an ensemble of eight simulations using the Rossby Centre Atmosphere model version 3 (RCA3) driven with lateral boundary data from global climate models (GCMs) are compared with results from a downscaled ERA40 simulation and gridded observations from 1980 –2006. The results showed that data from RCA3 scenario simulations should not be used as forcing for Baltic Sea models in climate change impact studies because biases of the control climate significantly affect the simulated changes of future projections. For instance, biases of the sea ice cover in RCA3 in the present climate affect the sensitivity of the model's response to changing climate due to the ice-albedo feedback. From the large ensemble of available RCA3 scenario simulations two GCMs with good performance in downscaling experiments during the control period 1980–2006 were selected. In this study, only the quality of atmospheric surface fields over the Baltic Sea was chosen as a selection criterion. For the greenhouse gas emission scenario A1B two transient simulations for 1961 –2100 driven by these two GCMs were performed using the regional, fully coupled atmosphere-ice-ocean model RCAO. It was shown that RCAO has the potential to improve the results in downscaling experiments driven by GCMs considerably, because sea surface temperatures and sea ice concentrations are calculated more realistically with RCAO than when RCA3 has been forced with surface boundary data from GCMs. For instance, the seasonal 2 m air temperature cycle is closer to observations in RCAO than in RCA3 downscaling simulations. However, the parameterizations of air-sea fluxes in RCAO need to be improved.

1. Introduction

Within the recently performed Baltic Sea Experiment (BALTEX) Assessment of Climate Change for the Baltic Sea Basin (BACC 2008; see also http://www.baltex-research.eu/BACC) it was concluded that 'identified trends in temperature and related variables (during the past 100 years) are consistent with regional climate change scenarios prepared with climate models'. BACC enjoyed active contributions by more than 80 scientists, and the BACC material was used by the Helsinki Commission (HELCOM) for its own climate assessment report of the Baltic Sea (http://www.helcom.fi). Regional climate model (RCM) results suggest that global warming may cause increased water temperatures of the Baltic Sea, reduced sea ice cover, possibly increased winter mean wind speeds causing increased vertical mixing, and possibly increased river runoff causing reduced salinity (BACC 2008). The projected hydrographic changes could therefore have significant impacts on the Baltic Sea ecosystem, e.g. species distributions, growth and reproduction of organisms including zooplankton, benthos and fish (e.g. MacKenzie et al. 2007). Unfortunately, the details have not been investigated thoroughly and, according to BACC, the complex response of the ecosystem is unknown.

First results from physical-biogeochemical modelling applying the so-called delta approach (e.g. Hay et al. 2000, Meier 2006) indicate that by the end of this century the impact of optimistic nutrient load reduction scenarios and the impact of climate change could be of the same order of magnitude in some regions of the Baltic Sea (Meier et al. 2011), emphasizing the urgent need to incorporate climate change into available decision support systems (DSSs). The DSS Nest (http://nest.su.se/nest) developed in the MARE program (http://www.mare.su.se) is today the only scientifically-based tool available to support the development of cost-effective measures against eutrophication for the entire Baltic Sea (Wulff et al. 2001, Savchuk & Wulff 2007, 2009). The Nest has been used to set the targets of the Baltic Sea Action Plan (BSAP, http://www.helcom.fi/stc/files/BSAP/BSAP_Final.pdf); however, the Nest does not take the effect of climate change (e.g. changing hydrography) into account.

In this study the first steps towards a DSS are described, which considers the combined effects of changing climate and changing nutrient loads on the Baltic Sea ecosystem. For this purpose a hierarchy of existing state-of-the-art, regional sub-models of the Earth system is applied (Figure 1). The atmospheric forcing for these regional sub-models is provided by an RCM, the Rossby Centre Atmosphere Ocean model (RCAO; Döscher et al. 2002), driven with boundary data from scenario simulations for the 21st century of Global Climate Models (GCMs). In these downscaling experiments, GCMs provide lateral boundary data and sea surface temperature (SST) and sea ice data for all sea areas of the model domain except for the Baltic Sea region, where atmosphere and ocean sub-models are interactively coupled.

Compared to earlier scenario simulations for the Baltic Sea, summarized by the BACC (2008), the downscaling approach is novel because

1. time-dependent (transient) scenario simulations from the present climate until 2100 are performed instead of selected time slices for present and future climates (e.g. Räisänen et al. 2004),
2. the uncertainties around these future projections are estimated using a multi-model approach comprising various coupled climate-environmental models for the Baltic Sea of differing complexity, and
3. improved model versions of the RCM and the GCMs are used.

Results from GCM scenario simulations described in the fourth Assessment Report of the Intergovernmental Panel on Climate Change (Solomon et al. 2007) are used as lateral forcing for RCAO. The DSS is built on the confidence of the models' capacity to simulate changing climate in the Baltic Sea region. By comparing the observed and simulated present climate, the predictive skills of the models are assessed and model uncertainties are

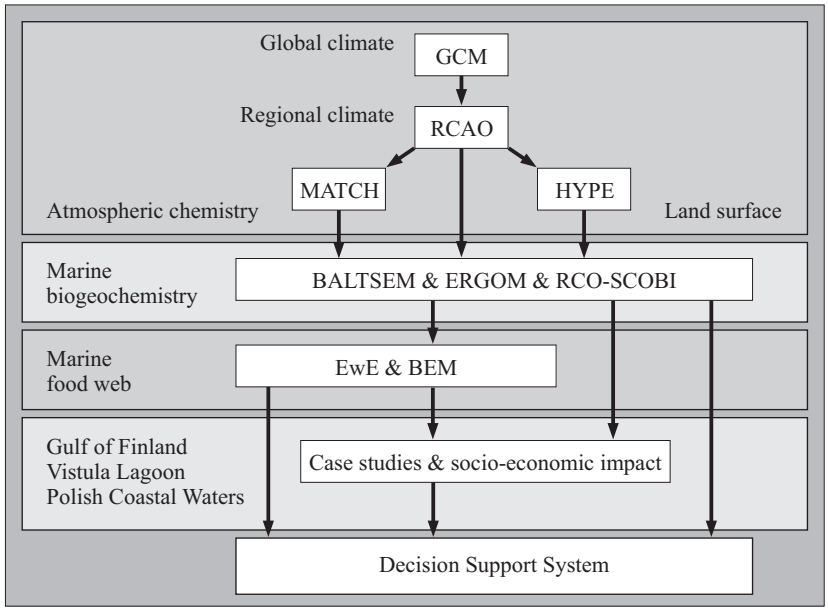

Figure 1. The envisaged decision support system is based upon information from scenario simulations from a regional, coupled atmosphere-ice-ocean-land surface model for the Baltic Sea catchment area, the Rossby Centre Atmosphere Ocean model (RCAO), forced with lateral boundary data from Global Climate Models (GCMs), a hydrological model to calculate river flow and nutrient loadings (HYPE, Hydrological Predictions for the Environment) and the Multi-scale Atmospheric Chemistry and Transport modelling system (MATCH), three marine physical-biogeochemical models of differing complexity for the Baltic Sea, food web and statistical fish population models, regional case studies and socio-economic impact studies. The scheme is highly simplified, neglecting complex interactions (e.g. fish predation pressure on zooplankton, socio-political changes that will affect climate and nutrient load scenarios). For further information the reader is referred to http://www.baltex-research.eu/ecosupport

quantified. We investigate the quality of atmospheric surface fields over the Baltic Sea from an ensemble of 16 RCM simulations recently performed at the Swedish Meteorological and Hydrological Institute, SMHI (Kjellström et al. 2011). Our approach is to select two out of eight available GCMs and two greenhouse gas emission scenarios to minimize the computational burden of the DSS simulations based upon the following criteria:

1. The downscaled atmospheric surface fields should have sufficiently high quality during the present climate to force coupled physical-environmental Baltic Sea models. The quality requirements are set

by the need for realistic model results of the present-day Baltic Sea climate.

2. The mini-ensemble still allows uncertainties caused by the GCMs and the emission scenarios to be estimated.

The high quality of the atmospheric surface fields is important because physical parameters have a large impact on the Baltic Sea ecosystem. Some functional dependences are even non-linear and include thresholds. For instance, water masses appropriate for the reproduction of cod should have salinities and oxygen concentrations larger than 11 PSU and 2 ml/l respectively (e.g. MacKenzie et al. 2007). The cod eggs sink until they reach waters of salinity of ca 11 PSU. If oxygen levels at the corresponding depth of neutral buoyancy (typically the depth of the permanent halocline in the south-western Baltic proper) are less than 2 ml/l, the eggs will not survive. Consequently, it is important to simulate both salinity and oxygen concentrations realistically.

Horizontal and vertical salinity variations in the Baltic Sea are large owing to the freshwater supply from the land. Sea surface salinities range from more than 20 PSU in the northern Kattegat to less than 2 PSU in the northern Bothnian Bay. As the Baltic Sea catchment area is four times larger than the Baltic Sea surface area, basically the difference between precipitation and evaporation over land controls the salinity gradients in the Baltic Sea. Thus, relatively small biases of simulated precipitation or evaporation over land in the RCM can have large impacts on salinity if the errors in precipitation and evaporation are not roughly equal, thus compensating each other. As a consequence, any shortcomings of the simulated water cycle may significantly affect the model results of cod reproduction in particular and the Baltic Sea ecosystem in general. Both coupled physical-biogeochemical and food web modelling requires high-quality atmospheric and hydrological forcing fields (Figure 1). Forcing biases could affect biodiversity and food web functioning, and in the worst case they might result in the complete loss of species and finally in a breakdown of the simulated food web.

As the marine ecosystem depends not only on mean hydrographical conditions but also on extremes, the variability of extreme variables needs to be simulated correctly by the RCM in addition to the mean states. Hence, the presented effort (as outlined in Figure 1) is a further development of earlier investigations based upon the delta approach, which assumes that the high-frequency variability of the atmospheric and hydrological forcing does not change (Meier 2006, Meier et al. 2011). Thus, it is important to select the applied GCMs carefully and to quantify uncertainties.

Biases of sea level pressure (SLP), air temperature, and precipitation over Europe's land area in GCM driven RCM simulations have been studied by Kjellström et al. (2011). They used the Rossby Centre Atmosphere model version 3 (RCA3; see Samuelsson et al. 2011) and found that biases during the control period are larger when RCA3 has been forced by GCMs compared to when it has been forced by so-called 'perfect' boundary conditions from reanalysis data. Typical biases over land in GCM driven simulations are up to 3–4°C for temperature and 100% for precipitation. Biases are to a large degree related to errors of the large-scale circulation, SSTs and sea ice cover in the GCMs. For surface air temperature the ensemble mean is generally better than the ensemble members.

In this study we focus on the assessment of atmospheric variables over the sea surface. Scenario results of the future marine environment and variables from the deeper ocean will be discussed elsewhere.

2. Methods

2.1. Regional climate simulations using RCA3

We use results from RCA3, which is a state-of-the-art regional atmosphere model including a land surface model (Samuelsson et al. 2006) and a lake model – PROBE (Ljungemyr et al. 1996, Jones et al. 2004, Samuelsson et al. 2011). For the present set-up SST and sea ice conditions are prescribed for all ocean areas within the chosen model domain, including the Baltic Sea (Figure 2).

Simulations with RCA3 use lateral boundary conditions from eight different GCMs (Table 1). All simulations are transient runs for 1961–2100. In addition to GCM-driven simulations, simulations with lateral boundary conditions and SST and sea ice from the ERA40 reanalysis data (Uppala et al. 2005) have also been used (Table 2). The reanalysis-driven simulations cover the time period 1961–2002. From August 2002 the simulations have been prolonged by using lateral boundary conditions from the operational analysis at the European Centre for Medium range Weather Forecasts (ECMWF). Most of the RCA3 simulations were performed with a horizontal grid resolution of 50 km. Owing to the computational burden only a few simulations could be performed with a 25 km resolution as well (Tables 1 and 2). For details of the available ensemble simulations and references to the GCMs, the reader is referred to Kjellström et al. (2011).

2.2. Coupled atmosphere-ocean simulations using RCAO

In addition to the RCA3 simulations, briefly introduced in the previous section, six dynamical downscaling experiments with the fully coupled,

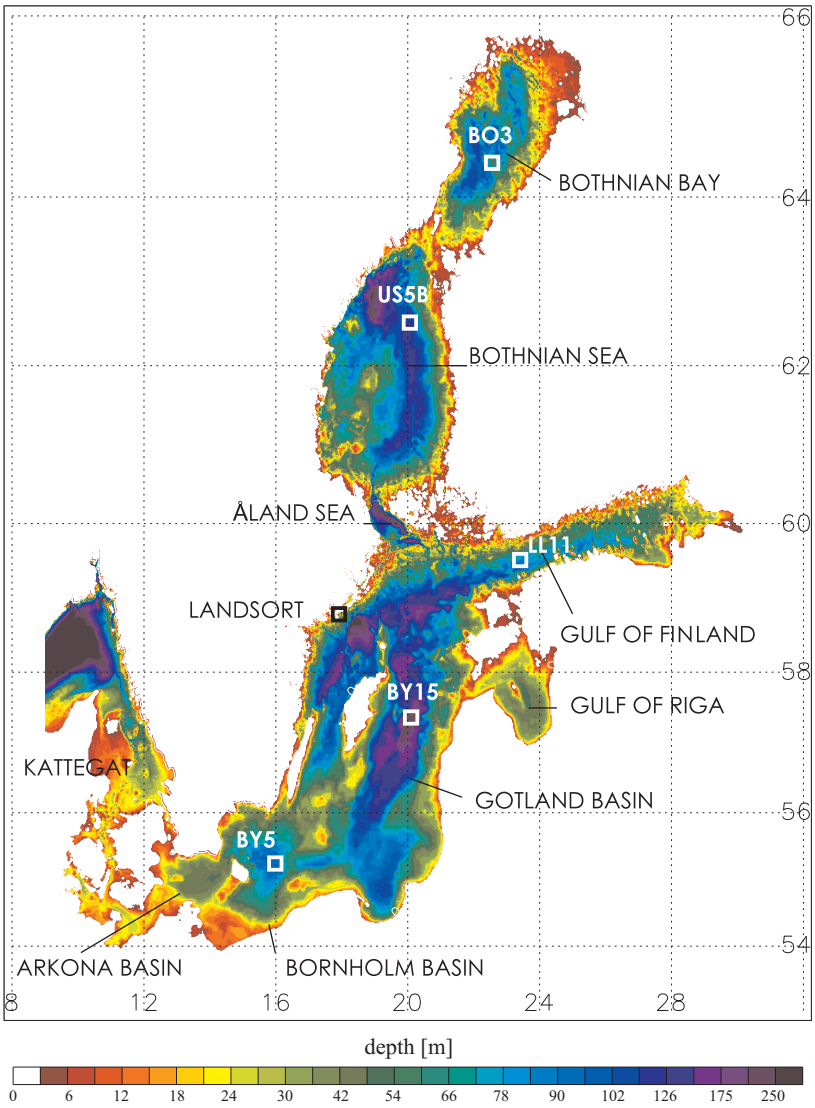

Figure 2. Bottom topography of the Baltic Sea (depths in m). The map shows the locations of the stations used for the model-data comparison in the Bornholm Deep (BY5), Gotland Deep (BY15), Gulf of Finland (LL11), Bothnian Sea (US5B) and Bothnian Bay (BO3). It also shows the location of the wind measurements at Landsort

atmosphere-ice-ocean-land surface model RCAO (the Rossby Centre Atmosphere Ocean model; see Döscher et al. 2002, 2010) were performed. In these experiments lateral boundary data from either ERA40 (Table 2) or two GCMs, HadCM3_ref and ECHAM5 (Table 1), were used.

Table 1. An overview of the RCM simulations with lateral boundary data from various GCMs. In this study the quality of the control climates 1980–2006 of the transient simulations 1961–2100 of the A1B emission scenario are analysed. The atmospheric part of the RCM (RCA3) has a horizontal resolution of either 25 or 50 km. Details are given in the text (section 2). ECHAM5 was used to simulate the A1B emission scenario three times, differing only in the initial conditions, to sample some of the natural variability. Here, we focus only on the third experiment (labelled 'r3' in Kjellström et al. 2011)

No.	RCM	GCM	Horizontal resolution of the atmosphere model
1	RCA3	ECHAM5 (MPI-met, Germany)	50 km
2	RCAO	ECHAM5 (MPI-met, Germany)	50 km
3	RCA3	ECHAM5 (MPI-met, Germany)	25 km
4	RCAO	ECHAM5 (MPI-met, Germany)	25 km
5	RCA3	ECHAM4 (MPI-met, Germany)	50 km
6	RCA3	HadCM3_ref (Hadley Centre, UK)	50 km
7	RCAO	HadCM3_ref (Hadley Centre, UK)	50 km
8	RCAO	HadCM3_ref (Hadley Centre, UK)	25 km
9	RCA3	HadCM3_low (Hadley Centre, UK)	50 km
10	RCA3	HadCM3_high (Hadley Centre, UK)	50 km
11	RCA3	Arpege (CNRM, France)	50 km
12	RCA3	CCSM3 (NCAR, USA)	50 km
13	RCA3	BCM (NERSC, Norway)	50 km

Table 2. Hindcast simulations for 1961–2007. Details are given in the text (section 2)

No.	RCM	GCM	Horizontal resolution of the atmosphere model
1	RCA3	ERA40 + ECMWF forecasts	50 km
2	RCA3	ERA40 + ECMWF forecasts	25 km
3	RCAO	ERA40 + ECMWF forecasts	50 km
4	RCAO	ERA40 + ECMWF forecasts	25 km

RCAO consists of the atmospheric component RCA3 (Samuelsson et al. 2011) and the oceanic component RCO (Meier et al. 2003) with horizontal grid resolutions of 25 and 11.1 km (six nautical miles) respectively. The ocean model consists of 41 vertical layers with layer thicknesses between 3 m close to the surface and 12 m at 250 m depth, which is the maximum depth in the model. For comparison with uncoupled RCA3 simulations, runs with a horizontal resolution of 50 km for the atmosphere were also performed (Table 2).

Within RCAO a recently developed river routing scheme provides the discharge from the land to the sea. The sea level elevation at the open boundary of the ocean model in the northern Kattegat is calculated from the simulated SLP difference across the North Sea between Oksøy in Norway and DeBilt in the Netherlands following the method by Gustafsson & Andersson (2001).

Two hindcast simulations for 1961–2007 and four transient simulations for 1961–2100 of RCAO driven with either reanalysis data, ECHAM5 or HadCM3_ref with two different horizontal resolutions (25 or 50 km) were performed (Tables 1 and 2). In the scenario simulations the greenhouse gas emission scenario A1B is assumed (Nakićenović et al. 2000).

2.3. Surface wind adjustment

Unfortunately, the majority of the ensemble simulations described in section 2.1 were performed with RCA3 using a horizontal resolution of 50 km only. For the purpose of wind speed modelling this horizontal resolution is not sufficient because the orography and the spatial land-sea distribution are not properly resolved. The impact of the horizontal resolution on the mean wind speed (without modification) is shown in Figure 3. Mean wind speeds over the Baltic Sea simulated with 25 km resolution are up to 60% larger than those simulated with 50 km resolution.

However, even with a horizontal resolution of 25 km wind speed is still underestimated in RCA3 and in many other RCMs (Rockel & Woth 2007). This is true both for mean wind speed and even more so for high wind speed extremes. Most often these high wind speed extremes are associated with wind gusts. Therefore, many RCMs have been equipped with gustiness parameterizations to better represent wind extremes. In RCA3 gustiness is calculated following the wind gust estimate method by Brasseur (2001), assuming that wind gusts develop when air parcels higher up in the boundary layer are deflected down to the surface by turbulent eddies (Nordström 2006).

According to Davis & Newstein (1968) the measured mean wind is the maximum 10-minute mean wind over the last three hours, and the measured wind gust is the maximum two second mean wind over the last 10 minute period. Observations indicate that the relationship between peak gusts and mean wind speeds is linear, suggesting an approximately constant factor of 1.6 at 10 m height (Davis & Newstein 1968). This observed relation between gusts and mean wind speed makes it possible to use output from the gustiness parameterization to adjust the simulated wind speed extremes.

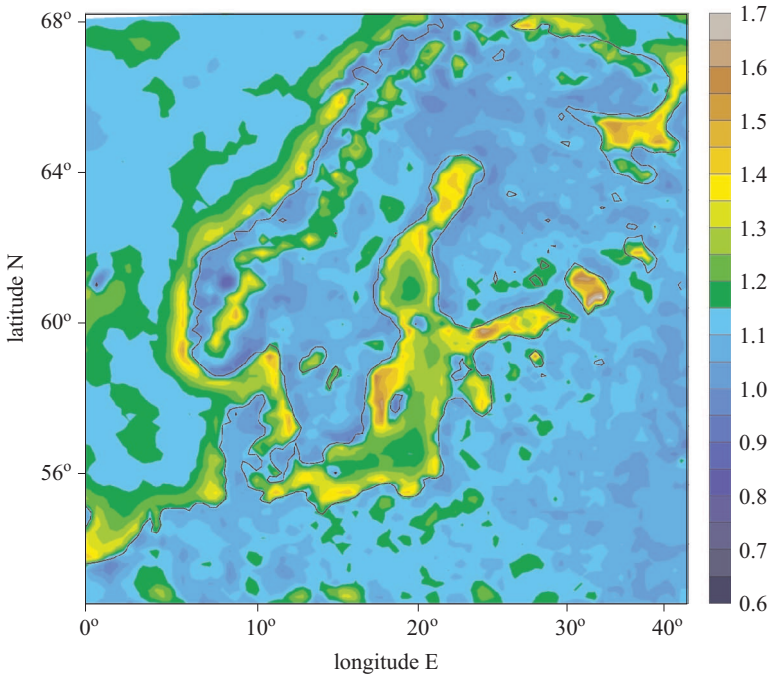

Figure 3. Linear regression coefficients between wind speeds during 1961–2007 simulated with RCA3-ERA40 using horizontal resolutions of 25 and 50 km

Thus, we modified the simulated mean wind speed at 10 m height U_{10}, utilizing simulated wind gusts U_{gust}, according to

$$U_{10}^{new} = \max(U_{gust}/1.6, U_{10}).$$

There is no adjustment for the wind direction. An example of the improvement is shown for the coastal station Landsort (Figure 4). Landsort is a well suited coastal station because for onshore winds (directions between 45 and 225°) the surrounding terrain causes relatively little disturbance. For further details of the method and results from other stations, the reader is referred to Höglund et al. (2009). These authors concluded that the wind statistics of the investigated coastal stations are clearly improved by the suggested modification. However, other quality measures like the root mean square error (RMSE) could deteriorate.

2.4. Validation data

Wind observations at coastal stations used for the development of the wind adjustment are described by Höglund et al. (2009) (see the previous section). In this study we focused on observations from Landsort for the

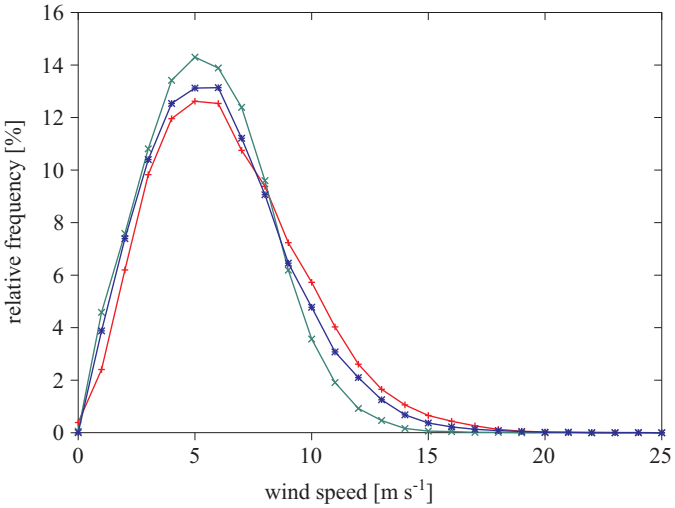

Figure 4. Relative frequency distribution (in %) of the wind speed (in m s^{-1}) at Landsort for the period 1996–2008: observations (red), mean wind speed simulated with RCA3 with a horizontal resolution of 25 km (green), and adjusted model wind using a gustiness parameterization (blue) (see simulation no. 2 in Table 2). For the location of the Landsort station, see Figure 2

period 1996–2008 after the recording switched from manual to automatic measurements (Figure 4).

Sea ice observations are compiled from BASIS – a data bank for Baltic sea ice and sea surface temperatures (Udin et al. 1981). The digital data base was constructed by extracting information from reanalysed ice and surface temperature maps from SMHI and the former Finnish Institute of Marine Research (today, the Finnish Meteorological Institute, FMI). Data are usually measured with a frequency of two maps per week during the ice season. The digital data were interpolated between measurements in order to obtain a daily time series for each year. When measurements were missing at the beginning (end) of the year, the first (last) available recording was used to fill in the dates for the daily time series. The data shown in the present study are from the years 1980 to 2008. From the sea ice concentration data, the ice extent was calculated by summing all the grid areas with a sea ice concentration greater than 10%.

At SMHI gridded SLP, 2 m air temperature, 2 m relative humidity and total cloud cover with a temporal resolution of three hours were compiled from observations since 1980 (e.g. Kauker & Meier 2003, Omstedt et al. 2005). In addition, 12 hourly accumulated precipitation fields are available at 06 and 18 UTC. Geostrophic wind speed was calculated and reduced to

10 m wind speed by using a varying factor in the range between 0.5 and 0.6, depending on the distance to the coast (Bumke & Hasse 1989). Note that mean 10 m wind speeds calculated from geostrophic wind fields very likely overestimate mean observed 10 m wind speeds.

Data from all available synoptic stations (about 700 to 800) covering the whole Baltic Sea drainage basin are interpolated on a 1° times 1° regular horizontal grid with respective latitude and longitude ranges of 50°N to 72°N and 8°E to 40°E. Thus, a two-dimensional univariate optimum interpolation scheme is utilized. Note that all stations are land-based: the data therefore suffer from a land-sea bias. For instance, air temperatures over the sea are expected to be slightly too high during summer and slightly too low during winter. However, the comparison between the ERA40 and the SMHI data bases suggests that the SMHI data also are of high quality over the sea (Omstedt et al. 2005). In the following we will refer to this gridded meteorological data set as the SMHI data.

2.5. Methods of comparison

We compared the results of RCA3 and RCAO simulations forced with GCM data at the lateral boundaries both with gridded observations from 1980–2006 and with RCA3 model results forced with so-called 'perfect' boundary data from the ERA40 re-analysis. The comparison was done at locations of oceanographic monitoring stations that characterize open sea conditions of the corresponding sub-basins (Figure 2). The results of the comparison do not differ significantly when instead of a single grid point the average of several contiguous grid points is considered.

As the resolution of the grid on which the SMHI observations are interpolated is rather coarse and as observations over the sea are sparse (only a few stations are located on islands), RCA3-ERA40 model results are not necessarily worse than SMHI data.

We focused on the analysis of the mean seasonal cycles at these stations, the interannual variability as expressed by the mean seasonal cycles of the corresponding standard deviations and on maps of the entire Baltic Sea area showing seasonal mean atmospheric and oceanic surface variables. The quantitative assessment of atmospheric surface fields is based upon mean biases of atmospheric surface variables at the five selected monitoring stations (Figure 2). We concentrated on variables that are necessary to force an ocean model, i.e. 2 m air temperature, 2 m specific humidity, SLP, adjusted wind speed, total cloudiness and precipitation.

3. Results

3.1. Hindcast simulations using RCA3-ERA40

Figure 5 shows the mean seasonal cycles and their variability of 2 m air temperature, SLP, adjusted 10 m wind speed, 2 m specific humidity, total cloudiness and precipitation over the Gotland Deep, characterizing open

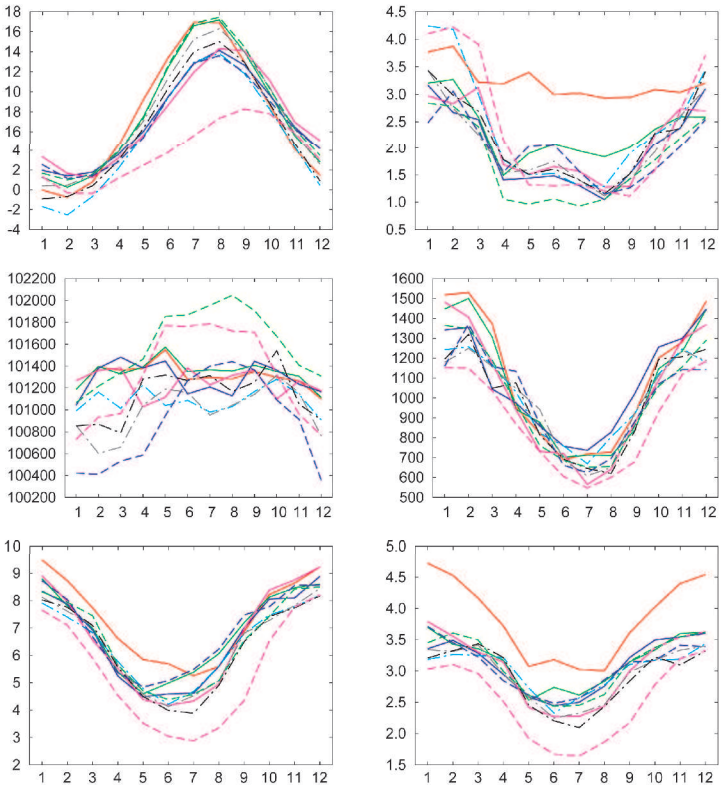

Figure 5. Monthly mean 2 m air temperature (in °C), sea level pressure (in Pa), adjusted 10 m wind speed (in m s^{-1}), specific humidity, total cloudiness, and precipitation (in mm day^{-1}) (left-hand column, top to bottom) and its corresponding monthly mean standard deviations (right-hand column) from the grid box closest to the Gotland Deep in the central Baltic proper for 1980–2006: SMHI data (solid red line), RCA3-ERA40 (solid green line), RCA3-ECHAM5 (solid blue line), RCA3-ECHAM4 (solid pink line), RCA3-HadCM3_low (dash-dotted light blue line), RCA3-HadCM3_high (dash-dotted grey line), RCA3-HadCM3_ref (dash-dotted black line), RCA3-Arpege (dashed green line), RCA3-CCSM3 (dashed blue line), and RCA3-BCM (dashed pink line). Note that all simulations were performed with RCA3 using a horizontal resolution of 50 km (Tables 1 and 2). The wind speed in all simulations was modified using simulated gustiness

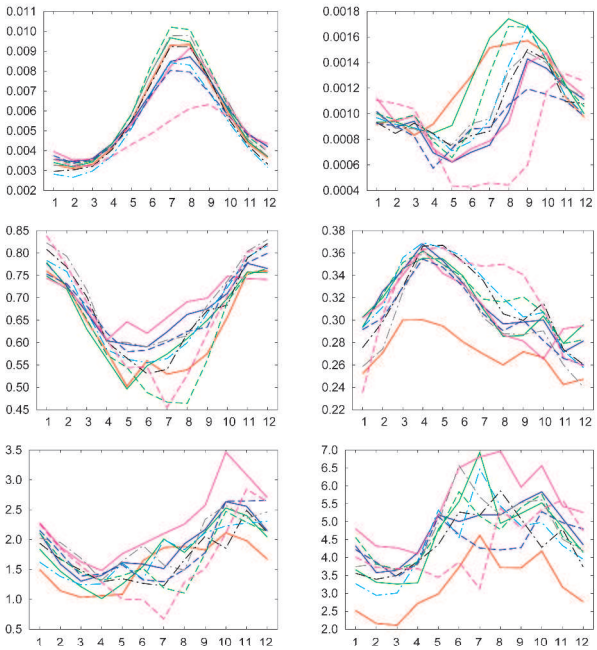

Figure 5. (*continued*)

sea conditions of the eastern Gotland Basin (see Figure 2). Qualitatively similar results were found in the other sub-basins. Further, Figures 6 and 7 show maps of winter mean SLP and of winter and summer mean 2 m air temperature for the entire Baltic Sea area respectively. The mean biases of five selected variables at five selected monitoring stations (Figure 2) are listed in Tables 3 to 7.

We found very good agreement between RCA3-ERA40 model results and the SMHI data for 2 m air temperature, SLP, cloudiness and precipitation (Figures 5 to 7 and Tables 3 to 7). Also, the horizontal distributions for SLP (Figure 6) and 2 m air temperature (Figure 7) in the RCA3-ERA40 simulation are close to the gridded observations. However, in winter RCA3 simulated land-sea temperature gradients are larger than observed values. In addition, simulated air temperatures over the sea are about 1°C higher in winter and about 1°C lower in summer than in the observations. Further, the interannual variability of the 2 m air temperature is smaller in the RCA3-ERA40 than in the SMHI data. These results could be explained by biases in the observational data set, because the SMHI data contain only observations from land.

The mean adjusted wind speed and its interannual variability are smaller in the RCA3-ERA40 than in the SMHI data (Figure 5). The largest annual

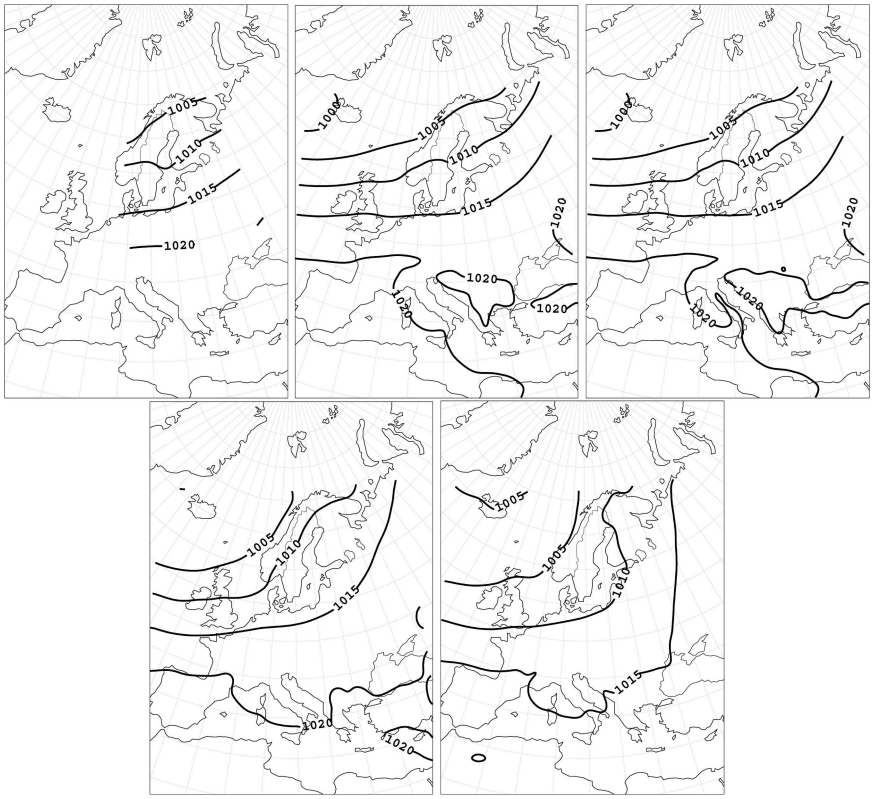

Figure 6. Maps of winter (December, January, February) mean sea level pressure (in hPa) for 1980–2006 from upper left to lower right: gridded observations, RCA3-ERA40, RCAO-ERA40, RCA3-ECHAM5 and RCA3-HadCM3_ref. The RCM simulations were performed with a 50 km horizontal resolution for the atmospheric model

mean biases are found in the northern Baltic Sea, where the simulated mean wind speed is underestimated by about 30% compared to the mean 10 m wind speed calculated from observations (Table 5). However, the annual mean bias averaged for all stations is smaller and amounts to about −16%.

In a previous study, Lind & Kjellström (2009) showed that simulated precipitation in RCA3 forced by ERA40 on the lateral boundaries agrees well with the high-resolution bias-corrected, gridded data set for precipitation by Rubel & Hantel (2001) during 1996–2000 (see also Kjellström & Lind 2009). Also, the annual mean net precipitation (precipitation minus evaporation) over land agrees well with the observed discharge for this region. Our results for the sea area support these earlier findings because RCA3-ERA40 results and SMHI data are in relatively good correspondence with monthly mean differences of less than about 20% (Figure 5).

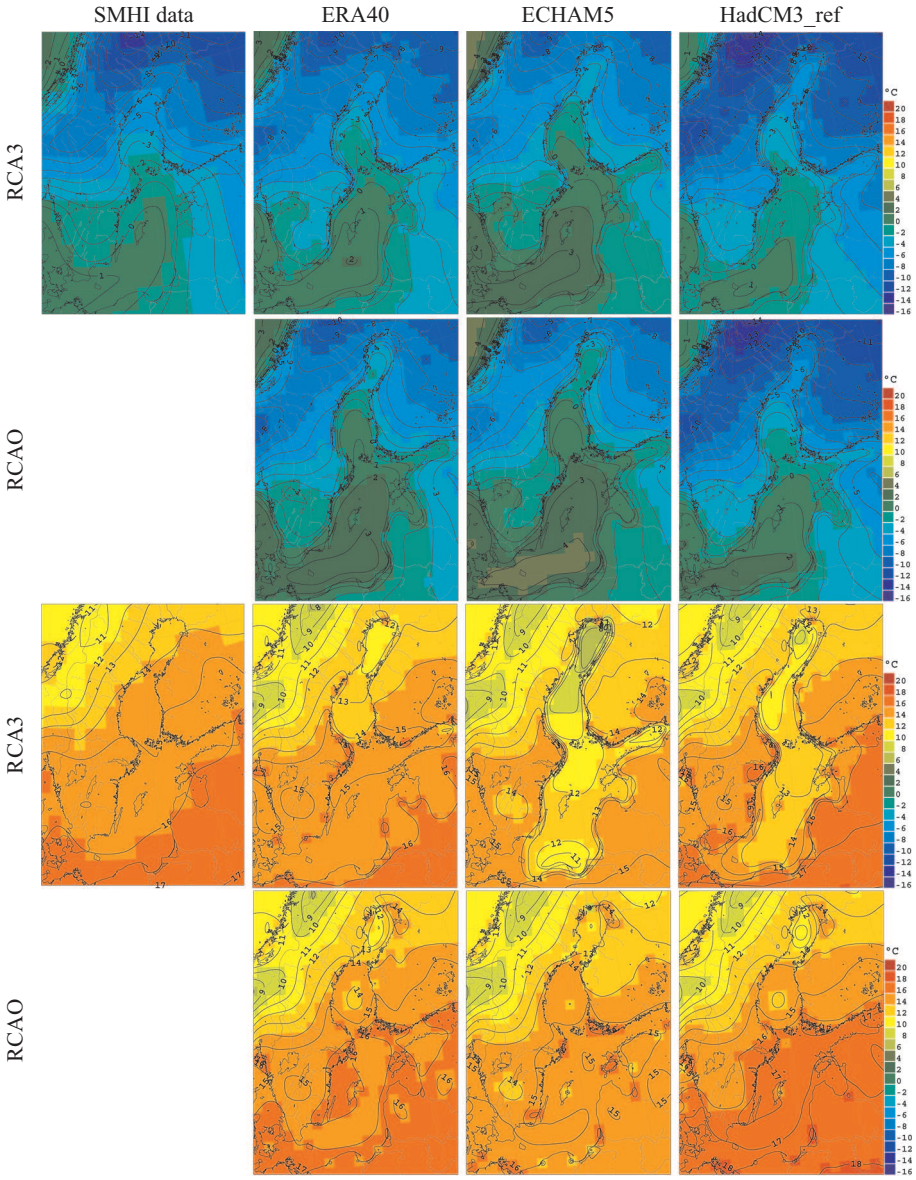

Figure 7. Maps of winter (December, January, February; upper panels) and summer (June, July, August; lower panels) mean 2 m air temperatures (in °C) for 1980–2006 in uncoupled (first and third row, except the first column) and coupled (second and fourth row) simulations using RCA3 and RCAO respectively: gridded observations (first column), RCA3/RCAO-ERA40 (second column), RCA3/RCAO-ECHAM5 (third column) and RCA3/RCAO-HadCM3_ref (fourth column). RCA3 and RCAO with a horizontal resolution of 50 km were used for the results shown

Table 3. Observed mean air temperature (in °C) and mean biases of RCA3 model simulations compared to gridded observations at five selected stations in the Baltic Sea. The locations of the stations are shown in Figure 2. Lateral boundary data of the RCA3 model simulations are either ERA40 or eight GCMs with a horizontal resolution of 50 km (see Table 1). Biases smaller than +/−1°C are highlighted with bold face numbers

	BO3	US5B	LL11	BY15	BY5	all
SMHI data	3.21	4.48	6.00	7.42	8.13	5.85
RCA3-ERA40	**− 0.78**	**−0.21**	**0.21**	**0.38**	**0.05**	**−0.07**
RCA3-ECHAM5	−1.33	**−0.19**	**−0.19**	**−0.36**	**−0.38**	**−0.49**
RCA3-ECHAM4	**0.07**	**0.04**	**−0.36**	**−0.14**	**0.17**	**−0.04**
RCA3-HadCM3_low	−2.67	−1.84	−2.10	−2.09	−1.73	−2.09
RCA3-HadCM3_high	**0.09**	**0.45**	**0.26**	**0.01**	**0.09**	**0.18**
RCA3-HadCM3_ref	−1.42	**−0.84**	−1.08	−1.17	**−0.88**	−1.08
RCA3-Arpege	**0.33**	**0.79**	**0.71**	**0.72**	**0.89**	**0.69**
RCA3-CCSM3	−1.06	−1.28	**−0.82**	**−0.64**	**−0.27**	**−0.81**
RCA3-BCM	−4.23	−3.66	−4.42	−3.61	−1.60	−3.50

Table 4. As Table 3 but for sea level pressure (in hPa). Biases smaller than +/−2 hPa are highlighted with bold face numbers

	BO3	US5B	LL11	BY15	BY5	all
SMHI data	1010.38	1010.93	1012.47	1013.12	1014.22	1012.22
RCA3-ERA40	**0.55**	**0.42**	**0.21**	**0.32**	**0.25**	**0.35**
RCA3-ECHAM5	**1.14**	**0.54**	**−0.13**	**−0.27**	**−0.60**	**0.13**
RCA3-ECHAM4	**−0.04**	**−0.46**	**−0.73**	**−0.63**	**−0.51**	**−0.47**
RCA3-HadCM3_low	**0.39**	**−0.36**	**−1.63**	−2.26	**−3.17**	**−1.41**
RCA3-HadCM3_high	**−1.36**	−2.05	−2.83	−3.21	−3.78	−2.65
RCA3-HadCM3_ref	**0.65**	**−0.14**	**−1.14**	**−1.77**	−2.81	**−1.04**
RCA3-Arpege	2.69	2.52	2.71	2.82	2.48	2.64
RCA3-CCSM3	−4.37	−4.87	−4.53	−4.15	−3.78	−4.34
RCA3-BCM	**1.55**	**0.69**	**0.40**	**−0.03**	**−1.39**	**0.24**

Table 5. As Table 3 but for the mean adjusted 10 m wind speed (in m s^{-1}) and its differences compared to the wind speed calculated from SLP from the SMHI data base (in %). Biases smaller than +/−20% are highlighted with bold face numbers

	BO3	US5B	LL11	BY15	BY5	all
SMHI data	6.67	6.24	6.84	7.32	7.32	6.88
RCA3-ERA40	−30.7	**−18.7**	**−17.8**	**−6.4**	**−7.5**	**−15.9**
RCA3-ECHAM5	−32.1	**−17.6**	**−19.1**	**−9.3**	**−7.0**	**−16.7**
RCA3-ECHAM4	−28.8	**−19.8**	−22.3	**−8.8**	**−3.2**	**−16.2**
RCA3-HadCM3_low	−24.8	**−14.1**	**−19.6**	**−11.8**	**−9.1**	**−15.7**
RCA3-HadCM3_high	−25.5	**−16.0**	**−19.7**	**−12.2**	**−10.5**	**−16.6**
RCA3-HadCM3_ref	−27.8	**−17.6**	−22.5	**−14.0**	**−11.3**	**−18.4**
RCA3-Arpege	**−16.3**	**−7.8**	**−16.3**	**−10.2**	**−9.8**	**−12.1**
RCA3-CCSM3	−30.5	−22.3	**−18.8**	**−5.8**	**5.5**	**−13.8**
RCA3-BCM	−34.2	−23.6	−37.6	−26.2	**−19.5**	−28.1

Table 6. As Table 3 but for cloudiness (between 0 and 1) and its biases (in %). Biases smaller than +/−10% are highlighted with bold face numbers

	BO3	US5B	LL11	BY15	BY5	all
SMHI data	0.63	0.64	0.67	0.63	0.62	0.64
RCA3-ERA40	**3.2**	**−1.6**	**−1.9**	**2.0**	**−2.2**	**−0.1**
RCA3-ECHAM5	**8.4**	**4.5**	**3.7**	**7.7**	**6.9**	**6.2**
RCA3-ECHAM4	10.7	**6.0**	**4.4**	**9.3**	**7.7**	**7.6**
RCA3-HadCM3_low	10.9	**4.3**	**0.2**	**6.4**	**5.4**	**5.4**
RCA3-HadCM3_high	14.5	**9.0**	**6.0**	10.7	**7.4**	**9.5**
RCA3-HadCM3_ref	11.3	**5.4**	**1.5**	**6.8**	**5.1**	**6.0**
RCA3-Arpege	**9.0**	**1.8**	**−3.8**	**−1.7**	**−5.2**	**−0.0**
RCA3-CCSM3	11.2	**5.7**	**3.7**	**7.0**	**7.5**	**7.0**
RCA3-BCM	18.8	11.0	**1.6**	**4.5**	**2.3**	**7.6**

Table 7. As Table 3 but for precipitation (in mm day^{-1}) and its biases (in %). Biases smaller than +/−15% are highlighted with bold face numbers

	BO3	US5B	LL11	BY15	BY5	all
SMHI data	1.45	1.58	1.71	1.57	1.54	1.57
RCA3-ERA40	**−4.6**	**−10.5**	**10.7**	**12.6**	**1.2**	**2.1**
RCA3-ECHAM5	**−0.4**	**1.8**	18.3	19.9	23.0	**12.8**
RCA3-ECHAM4	25.3	18.6	31.4	44.1	38.9	31.7
RCA3-HadCM3_low	**6.9**	**−3.1**	**−0.5**	**12.5**	**8.2**	**4.7**
RCA3-HadCM3_high	**14.5**	**8.6**	**14.6**	23.8	17.2	15.7
RCA3-HadCM3_ref	**7.9**	**−0.8**	**0.1**	**8.4**	**10.3**	**5.0**
RCA3-Arpege	17.3	**8.7**	**9.1**	**8.4**	**3.2**	**9.3**
RCA3-CCSM3	**3.4**	**−4.5**	**13.9**	17.8	22.1	**10.7**
RCA3-BCM	44.1	20.6	**6.8**	**6.2**	**4.4**	15.9

3.2. Control climate in RCA3-GCMs

We found relatively large biases of the simulated mean seasonal cycles and their interannual variability when RCA3 is driven by the GCMs listed in Table 1. RCA3-BCM in particular considerably underestimates inter alia the amplitude of the seasonal 2 m air temperature cycle. The maximum occurs in September and is more than 9°C smaller than the July maximum in RCA3-ERA40. Also, the other RCA3 simulations driven by GCMs underestimate both 2 m air temperature in summer and 10 m wind speed in summer and autumn (except CCSM3 for wind speed). All GCM driven simulations overestimate winter cloudiness. The summer biases are even larger and have positive or negative signs depending on the driving GCM. Most models overestimate precipitation over the sea although this problem seems to have improved considerably compared to earlier studies (Räisänen et al. 2004). For instance, the annual mean precipitation and the mean seasonal cycle of precipitation are much better simulated in RCA3-ECHAM5 than in RCA3-ECHAM4 (Figure 5, Table 7).

Although observed horizontal gradients of annual mean surface fields between sub-basins are reproduced by most models (not shown), we also found discrepancies. For instance, in ECHAM4 and ECHAM5 driven simulations the mean SLP and the SLP gradient between the northern and southern Baltic Sea are well simulated, indicating a realistic large-scale circulation in these models; in contrast, in all HadCM3 driven simulations, regardless of the HadCM3 version used (HadCM3_ref, HadCM3_low, HadCM3_high), the gradient is significantly underestimated, with SLP too low in the southern Baltic (for HadCM3_ref, see Figure 6; HadCM3_low and HadCM3_high are not shown). The largest SLP biases are found in the BCM driven simulation. Although SLP biases are the smallest in ECHAM5 driven RCA3 simulations, winds over the Baltic Sea have an artificial meridional component (Figure 6). The impacts of either horizontal resolution (25 or 50 km) or of the chosen RCM (RCA3 or RCAO) on SLP results is small compared to the impact of the lateral boundary data from various GCMs.

In RCA3-ECHAM5 and RCA3-HadCM3_ref summer 2 m air temperatures are much too low (Figure 7). On the other hand, winter 2 m air temperatures are too high in RCA3-ECHAM5 but reasonably well reproduced in RCA3-HadCM3_ref (except a slightly cold bias in the Baltic proper).

In summary, mean biases of 2 m air temperature (Table 3), SLP (Table 4), SLP gradients (Figure 6), cloudiness (Table 6) and precipitation (Table 7) are usually larger when RCA3 is forced by GCMs than when it is forced by ERA40 data. Exceptions are the smaller biases of 2 m air

temperature in RCA3-ECHAM4, of SLP in RCA3-ECHAM4 and in RCA3-BCM, and of cloudiness in RCA3-Arpege. The mean biases of adjusted wind speed are slightly smaller in RCA3-HadCM3_low, RCA3-Arpege and RCA3-CCSM3 than in RCA3-ERA40 (Table 5).

Although during the control period 1980–2006 none of the investigated models is best in terms of the mean absolute errors of all atmospheric surface variables, the assessment suggests that ECHAM5 and HadCM3_ref driven RCA3 simulations belong to the group of models with a better performance (Tables 3 to 7). Hence, in the following we focus on these two GCMs.

3.3. RCA3 versus RCAO

Figure 8 shows the mean seasonal cycles of 2 m air temperature over the Gotland Deep in RCA3 and RCAO simulations with the 25 and 50 km resolutions forced with ERA40, ECHAM5 and HadCM3_ref. In summer RCA3 and RCAO simulations forced with ERA40 data result in mean 2 m air temperatures close to the observed values (see also Figure 7). However, in winter RCAO is too warm. The bias is largest in the northern part of the Baltic (Figure 7), which is usually covered with sea ice, indicating shortcomings of the air-sea fluxes in RCAO during winter. There is a small dependence on the horizontal resolution. The winter mean 2 m air temperature is better simulated with the 25 than with the 50 km horizontal resolution (Figure 8), perhaps because of the more realistic land-sea mask in the high-resolution simulation.

In the hindcast simulation using RCAO-ERA40 (50 km) the results for sea ice extent are relatively close to the observations available for the period 1980–2008 (Figure 9, upper panels). The sea ice model of RCAO slightly underestimates the seasonal ice cover with too small an annual maximum ice extent.

Both GCM driven RCA3 simulations are too cold in summer (Figures 7 and 8). In winter RCA3-ECHAM5 is too warm and RCA3-HadCM3_ref is slightly too cold compared to RCA3-ERA40 with 'perfect' lateral and surface boundary conditions. The utilization of RCAO very much improves the results in summer in ECHAM5 driven simulations, but not in winter, when the air temperatures are still too high. As the large-scale circulation in ECHAM5 is too zonal (Kjellström et al. 2011), warm air is advected from the North Atlantic into the Baltic Sea region, causing a lack of sea ice and excessively high 2 m air temperatures.

In HadCM3_ref driven simulations we found in principle similar results (Figures 7 and 8). When RCAO is used to downscale the GCM data, summer 2 m air temperatures are closer to reality than in RCA3-HadCM3_ref. However, now the air temperatures are slightly too high over

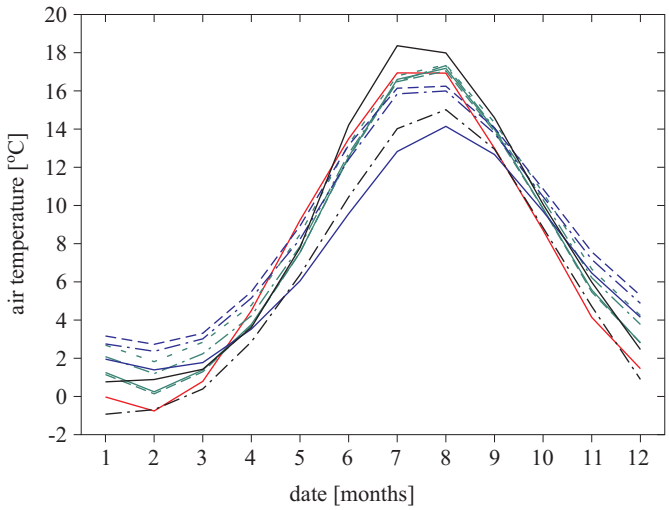

Figure 8. Monthly mean 2 m air temperature (in °C) over the Gotland Deep (BY15) in the central Baltic proper for 1980–2006: SMHI data (solid red line), RCA3-ERA40 50 km (solid green line), RCA3-ERA40 25 km (dashed green line), RCAO-ERA40 50 km (dotted green line), RCAO-ERA40 25 km (dash-dotted green line), RCA3-ECHAM5 50 km (solid blue line), RCAO-ECHAM5 50 km (dashed blue line), RCAO-ECHAM5 25 km (dash-dotted blue line), RCA3-HadCM3_ref 50 km (dash-dotted black line), and RCAO-HadCM3_ref 50 km (solid black line)

the Gotland Deep during summer but relatively close to the SMHI data during winter. Overall, the resolution has a minor impact on the quality of surface air temperatures, although some differences during winter were found, as mentioned above (Figure 8). However, RCAO has the potential to improve air temperature over the sea in all Baltic sub-basins at least during summer, when the westerly flow over the North Atlantic is generally weaker than during winter (Kjellström et al. 2005). In winter, air temperatures in the region are perhaps controlled more by the large-scale circulation, which is determined by the lateral rather than the surface boundary conditions from the GCM. A more realistic representation of SST and sea ice cover with the help of the high-resolution ocean model in RCAO has a minor impact on air temperatures in winter but a major impact during spring and summer (see also the next sub-section).

During 1980–2007 sea ice discrepancies between RCAO-ECHAM5 and observations are larger than biases in RCAO-ERA40 (Figure 9, middle panels). Owing to the warm bias in RCAO-ECHAM5 the mean maximum sea ice extent is only about 60% of the observed value, even though it is within the range of natural variability. On the other hand, the mean seasonal ice cover calculated with atmospheric forcing from RCAO-HadCM3_ref is

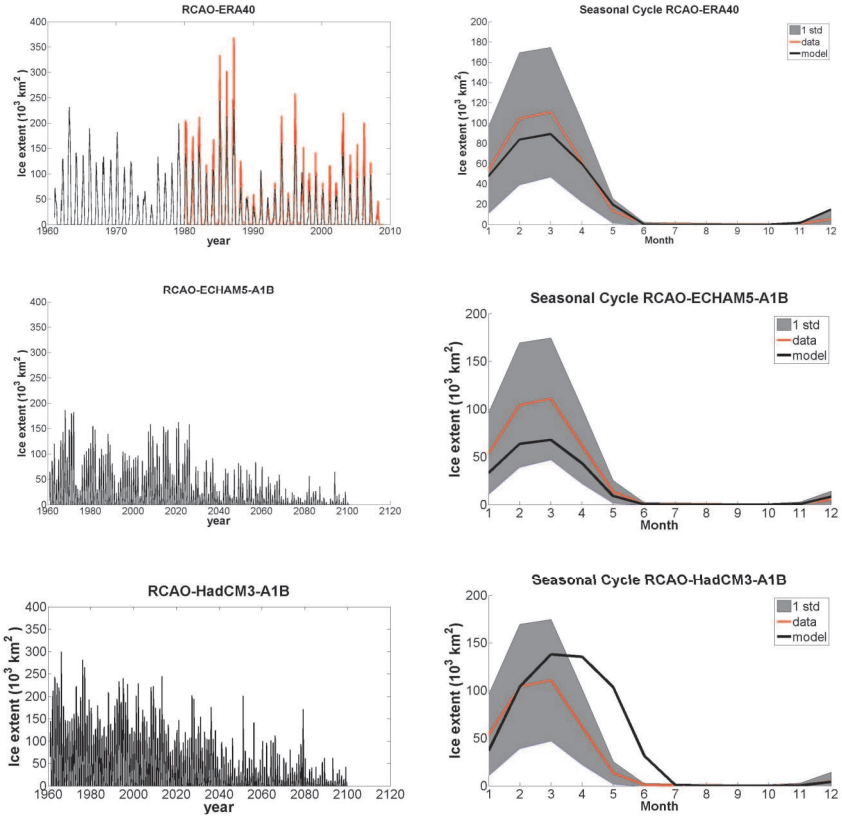

Figure 9. Sea ice covered area (in km^2) as a function of time for 1961–2007 and 1961–2100 in hindcast and scenario simulations respectively (left-hand panels): observations (red), model results (black). The mean seasonal cycles for 1980–2007 are also shown (right-hand panels). The three rows of panels show results from RCAO-ERA40 (upper panels), RCAO-ECHAM4 A1B (middle panels) and RCAO-HadCM3_ref A1B (lower panels) using a horizontal resolution of 50 km for the atmosphere model

overestimated compared to observations (Figure 9, lower panels). In this simulation the largest biases occur in spring owing to the delayed melting of the ice cover.

3.4. Scenario simulations

Depending on the season and location, simulated 2 m air temperature changes over the Baltic Sea in the selected scenario simulations, RCAO-ECHAM5 A1B and RCAO-HadCM3_ref A1B, are in the range between +1 and +7°C (Figure 10). 2 m air temperature changes are largest over the

northern Baltic Sea during all seasons. Similar results are found in RCA3-ECHAM5 A1B and RCA3-HadCM3 A1B simulations but with somewhat smaller air temperature increases in the northern Baltic Sea (Figure 10).

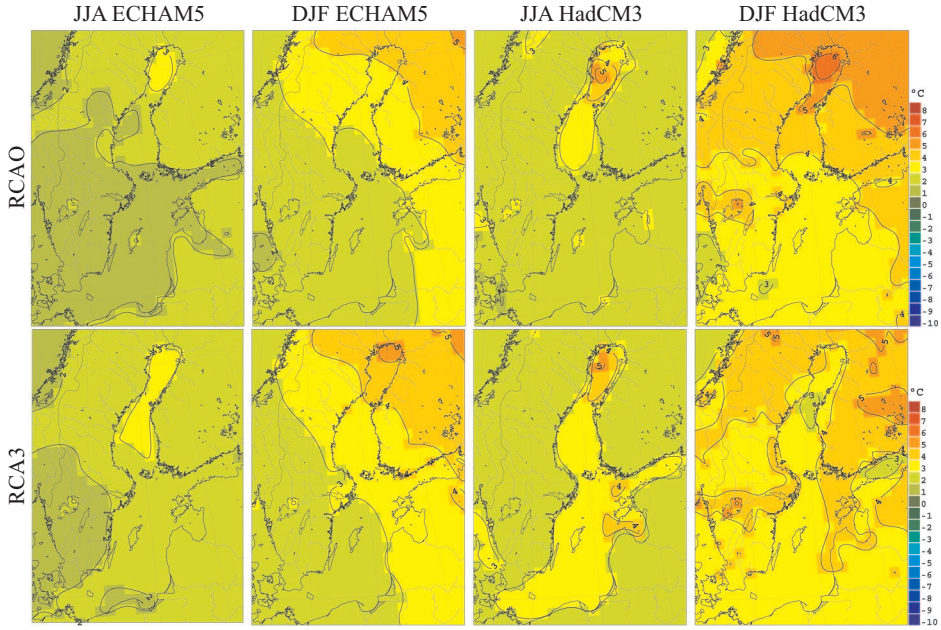

Figure 10. Maps of winter (December, January, February; second and fourth column) and summer (June, July, August; first and third column) mean 2 m air temperature changes (in °C) between 2061–2090 and 1970–1999 in the A1B scenario in RCAO (upper row) and in RCA3 (lower row) using a horizontal resolution of 50 km. Downscaled results using ECHAM5 (first and second column) and HadCM3_ref (third and fourth column) are depicted

Over land the surface air temperature changes are largest during winter (Figure 10; cf. Kjellström et al. 2011). This warming pattern with a maximum in the north-eastern model domain of RCAO, most notably in northern Fennoscandia, the Kola Peninsula and the ocean areas close to the northern rim (not shown), is explained by the increased zonality of the mean SLP field together with the snow-albedo feedback over land (Kjellström et al. 2011). In summer SLP changes are small and there is no impact of the snow-albedo feedback. This leads to relatively small changes in surface air temperature. The outstanding role of the Baltic Sea for changes in surface variables like air temperature is explained by the sea ice – albedo feedback as explained below.

As the same greenhouse gas emission scenario (A1B) is assumed, differences in the simulated changes depend on the forcing GCM (ECHAM5

or HadCM3_ref) and on the RCM (RCAO or RCA). Air temperature changes in HadCM3_ref driven RCAO scenario simulations are greater than in ECHAM5 driven RCAO simulations, with the largest differences being over the northern Baltic Sea during winter and spring (about 2°C) (Figure 10). During the same seasons the differences between RCAO and RCA3 with HadCM3_ref forcing are also the largest. The uncertainty could be explained by the biases of the control climate and the related reduction of the sea ice – albedo feedback. Because of the winter warm bias in ECHAM5 driven simulations during the control period (Figure 7), sea ice concentration and thickness are reduced in the present climate (Figure 9), such that in the future climate the increased warming effect of the sea ice – albedo feedback is artificially reduced. The mean ice cover reduction is larger in RCAO-HadCM3_ref A1B than in RCAO-ECHAM5 A1B (Figure 9).

At the end of the 21st century fairly severe winters will still be found in RCAO-HadCM3_ref A1B, whereas all winters are mild in RCAO-ECHAM5 A1B (Figure 9), but in neither simulation will any winter be completely ice free by the end of this century.

Regional details of the sea ice cover are more realistically simulated in RCAO than in most GCMs, which suffer from their coarser horizontal resolution (not shown). Consequently, 10 m wind speed changes in areas of reduced sea ice cover are larger in RCAO than in RCA3 simulations (Figure 11, upper panels) because of the increased SSTs and the related reduced static stability of the planetary boundary layer, PBL (cf. Meier et al. 2006). For instance, in the Bothnian Bay maximum winter mean 10 m wind speed changes over the sea of about 1 m s^{-1} are found in RCAO-HadCM3_ref A1B. Both 10 m mean wind speed and gustiness increase during winter as a result of the changing stability (Figure 11, lower panels). Changes during the other seasons are statistically not significant (not shown). In the RCA3-ECHAM5 A1B simulation wind and gustiness changes are statistically not significant at all seasons (not shown).

The ice albedo – feedback affects both air temperature and SST changes between future and present climates. Figure 12 shows seasonal mean SST changes in RCAO-HadCM3_ref A1B and RCAO-ECHAM5 A1B. The largest SST changes are found during spring in the Bothnian Sea and Gulf of Finland and during summer in the Bothnian Bay. If the ice cover does not vanish completely from the Bothnian Sea, the ice will at least melt here earlier during spring (from March to May). Hence, the largest SST response during spring is expected to occur in the Bothnian Sea. Later during summer (from June to August, with June being the most important month), the ice cover will also retreat in the Bothnian Bay, causing the maximum SST increase to shift northwards from the Bothnian Sea into the

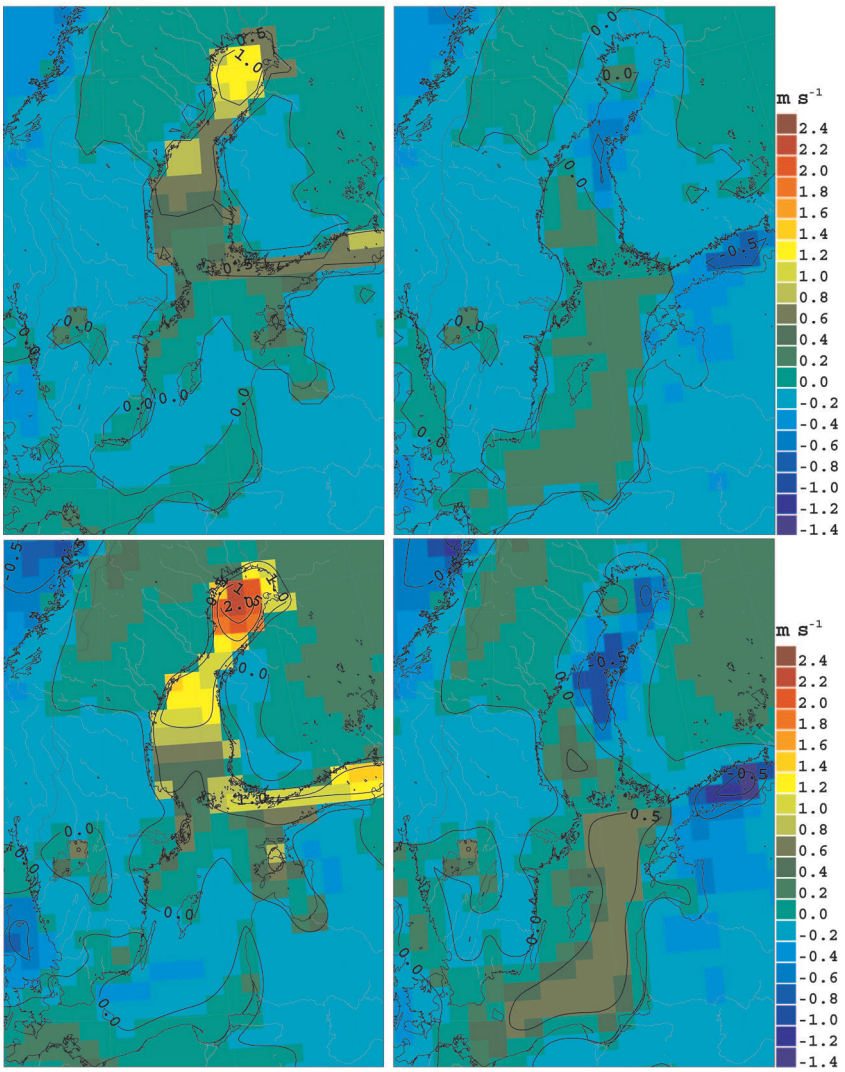

Figure 11. Winter (December, January, February) mean corrected 10 m wind speed changes (in m s^{-1}) (upper panels) and gustiness changes (in m s^{-1}) (lower panels) for 2061–2090 and 1970–1999 simulated with RCAO-HadCM3_ref A1B (left-hand panels) and RCA3-HadCM3_ref A1B (right-hand panels) with a 50 km horizontal resolution

Bothnian Bay. Maximum SST changes amount to about 4°C and 8°C in RCAO-ECHAM5 A1B and RCAO-HadCM3_ref A1B respectively.

For precipitation changes we refer to the studies by Kjellström & Lind (2009) and Kjellström et al. (2011). As the freshwater supply from precipitation minus evaporation over sea amounts to only ca 11% (Meier

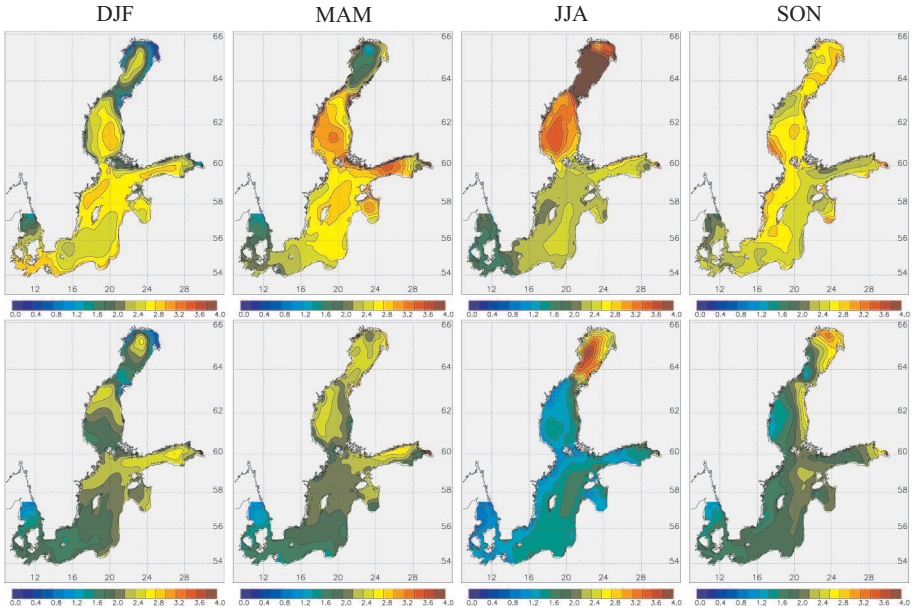

Figure 12. Seasonal mean sea surface temperature changes (in °C) for 2061–2090 and 1970–1999 in RCAO-HadCM3_ref A1B (upper panels) and RCAO-ECHAM5 A1B (lower panels). From left to right the columns show the respective changes for winter (December to February, DJF), spring (March to May, MAM), summer (June to August, JJA) and autumn (September to November, SON). Changes larger than 4°C are shown in brown

& Döscher 2002), it is basically the changes in the hydrological cycle over land that will control the future salinity of the Baltic Sea (in addition to possible wind speed changes, e.g. Meier 2006). According to Kjellström et al. (2011), precipitation increases during winter in the north and decreases during summer in the south. However, the borderline migrates back and forth from a northerly position in summer to a southerly one in winter. The precipitation increase is partly explained by increased zonality and partly by an amplification of the hydrological cycle, as Kjellström & Lind (2009) found.

4. Discussion

According to Kjellström et al. (2011), the explained variance based upon spatial variances of SLP and the mean absolute error for temperature and precipitation over land suggest that RCA3 driven with the GCMs Arpege, ECHAM5 (experiment '-r3', for the description see Kjellström et al. 2011), HadCM3_ref and HadCM3_low perform best during the control period. However, in winter all GCM simulations are too zonal, thus affecting the

quality of the other variables due to advection. Focusing on the atmospheric surface fields over sea, our analysis confirms the results by Kjellström et al. (2011). However, it is impossible to rank the models. Depending on the variable, the results are quite different. For instance, ECHAM5 and HadCM3_ref driven simulations showed the best SLP and air temperature results, respectively, but none of the models is perfect for all variables.

In addition to biases of the large-scale circulation induced by the lateral boundary data, atmospheric surface variables over sea also suffer from biases of SST and sea ice data from the GCMs. Therefore, the results of RCA3 could be affected such that the gain of the higher resolution in the RCM is compensated for by these biases. A quality assessment of atmospheric fields from RCA3 over the sea is more a validation of GCM results for the Baltic Sea than an evaluation of RCA3 performance.

Hence, in this study the added value of the coupled atmosphere-ice-ocean model RCAO was investigated. Because of the computational burden we performed transient simulations with only two different driving GCMs selected from the group of models with better performance. We showed that the results from both downscaling experiments improved the 2 m air temperature over the sea during summer but not necessarily during winter. The latter finding was explained by the impact from the lateral boundary data. However, further downscaling experiments with other GCMs are necessary to illuminate the impact from various data sets. In addition, it is important to note that further model development to improve RCAO is necessary. We identified too low a wind speed over sea (although the higher resolution improved the situation) and too high an air temperature over ice covered areas, suggesting perhaps the shortcomings of incoming long-wave radiation during winter.

A detailed analysis of the future ocean climate in the transient simulations lies beyond the scope of this study and will be presented in forthcoming publications.

5. Conclusions

The following conclusions were drawn from the simulations:

1. We found that in RCA3 simulations driven by eight GCMs (with one exception) the mean seasonal cycles of atmospheric variables, like 2 m air temperature, SLP, 10 m wind speed, 2 m specific humidity, total cloudiness and precipitation over the Baltic Sea, their variability and mean north-south gradients, are qualitatively well simulated. However, a detailed, quantitative assessment showed that the biases are considerable. In most simulations 2 m air temperatures are underestimated during summer and overestimated during winter.

During all seasons the 10 m wind speed is underestimated partly because of the horizontal resolution of the atmospheric model RCA3 of 50 km, which is too coarse for the Baltic Sea region. Although the positive precipitation bias is significantly improved compared to earlier downscaling experiments when the latest versions of RCA3 and of the GCMs were used, the annual mean precipitation in most of the GCM driven simulations is still overestimated. Given the above-mentioned biases, and as RCA3 in dynamical downscaling experiments makes use of SST and sea ice data from the GCMs, which suffer from the coarse resolution, the results of the RCA3 scenario simulations should not be used as forcing for Baltic Sea models.

2. We obtained significantly improved results for the 10 m wind speed over the open sea with an increased horizontal resolution of 25 compared to 50 km in RCA3. To correct the remaining biases of the wind speed in the 25 km simulations, a statistical adjustment based on simulated gustiness was tested, leading to satisfactory results. For the other atmospheric variables the increased resolution had less impact and no further adjustment was needed.
3. Atmospheric surface variables over the Baltic Sea from the fully coupled RCAO model forced with 'perfect' boundary conditions from ERA40 are very close to the corresponding RCA3 results when SST and sea ice concentration from observations are used as surface boundary conditions. The results are also close to observations from the SMHI data base. However, in RCAO we found a winter warm bias of the 2 m air temperature in the northern sub-basins. Hence, in future work the air-sea fluxes in RCAO need to be improved.
4. In the simulations forced with either ECHAM5 or HadCM3_ref, summer 2 m air temperatures during the control period are better simulated with RCAO than with RCA3. A more realistic SST representation in RCAO with the help of the high-resolution ocean model explains this improvement. However, the winter warm bias in ECHAM5 driven RCA3 simulations could not be compensated for with the help of RCAO. On the contrary, winter mean 2 m air temperatures over the northern part of the Baltic Sea are even warmer in RCAO than in RCA3 simulations because of the shortcomings of RCAO over sea ice that occur even with 'perfect' boundary conditions, as mentioned above. In winter the climate of the Baltic Sea region is very much controlled by the large-scale atmospheric circulation. As in ECHAM5 the circulation is too zonal: warm air is advected from the North Atlantic into the Baltic Sea region producing too high 2 m air temperatures and too little sea ice.

5. Results of future projections depend on the forcing GCM and on the RCM (RCAO or RCA3). Some differences between RCAO and RCA3 are explained by biases of the control climate in the GCMs. For instance, the winter warm bias in ECHAM5 causes a reduced sea ice – albedo feedback and consequently a smaller warming of the Baltic Sea than in HadCM3_ref driven simulations. Other differences are explained by more realistically simulated air-sea fluxes in RCAO. For instance, 10 m wind changes are larger in RCAO than in RCA3 simulations because of increased SSTs and reduced stability of the PBL in areas of reduced sea ice cover.

In summary, it is important to develop fully coupled atmosphere-ice-ocean models with high quality in present climate simulations to avoid the impact of biases on model sensitivity in climate change simulations.

Acknowledgements

We thank our colleagues at SMHI, Anders Ullerstig and Ulf Hansson, for their technical support in performing the RCA3 and RCAO simulations respectively.

References

BACC – BALTEX Assessment of Climate Change, 2008, *Assessment of climate change for the Baltic Sea basin*, The BACC Author Team, Reg. Clim. Stud. Ser., Springer, Berlin, Heidelberg, 474 pp.

Brasseur O., 2001, *Development and application of a physical approach to estimating wind gusts*, Mon. Weather Rev., 129 (1), 5–25.

Bumke K., Hasse L., 1989, *An analysis scheme for the determination of true surface winds at sea from ship synoptic wind and pressure observations*, Bound.-Lay. Meteorol., 47 (1–4), 295–308.

Davis F. K., Newstein H., 1968, *The variation of gust factors with mean wind speed and with height*, J. Appl. Meteorol., 7 (3), 372–378.

Döscher R., Willén U., Jones C., Rutgersson A., Meier H. E. M., Hansson U., Graham L. P., 2002, *The development of the regional coupled ocean-atmosphere model RCAO*, Boreal Environ. Res., 7, 183–192.

Döscher R., Wyser K., Meier H. E. M., Qian M., Redler R., 2010, *Quantifying Arctic contributions to climate predictability in a regional coupled ocean-ice-atmosphere model*, Clim. Dynam., 34 (7–8), 1157–1176.

Gustafsson B. G., Andersson H. C., 2001, *Modeling the exchange of the Baltic Sea from the meridional atmospheric pressure difference across the North Sea*, J. Geophys. Res., 106 (C9), 19 731–19 744.

Hay L. E., Wilby R. L., Leavesley G. H., 2000, *A comparison of delta change and downscaled GCM scenarios for three mountainous basins in the United States*, J. Am. Water Resour. As., 36 (2), 387–398.

Höglund A., Meier H. E. M., Broman B., Kriezi E., 2009, *Validation and correction of regionalised ERA-40 wind fields over the Baltic Sea using the Rossby Centre Atmosphere model RCA3.0.*, Rap. Oceanogr. No. 97, SMHI, Norrköping, 29 pp.

Jones C. G., Willén U., Ullerstig A., Hansson U., 2004, *The Rossby Centre regional atmospheric climate model (RCA). Part I: Model climatology and performance characteristics for present climate over Europe*, AMBIO, 33 (4–5), 199–210.

Kauker F., Meier H. E. M., 2003, *Modeling decadal variability of the Baltic Sea: 1. Reconstructing atmospheric surface data for the period 1902–1998*, J. Geophys. Res., 108 (C8), 3267, doi: 10.1029/2003JC001797.

Kjellström, E., Döscher R., Meier H. E. M., 2005, *Atmospheric response to different sea surface temperatures in the Baltic Sea: coupled versus uncoupled regional climate model experiments*, Nord. Hydrol., 36 (4–5), 397–409.

Kjellström E., Lind P., 2009, *Changes in the water budget in the Baltic Sea drainage basin in future warmer climates as simulated by the regional climate model RCA3*, Boreal Environ. Res., 14 (1), 114–124.

Kjellström E., Nikulin G., Hansson U., Strandberg G., Ullerstig A., 2011, *21st century changes in the European climate: uncertainties derived from an ensemble of regional climate model simulations*, Tellus A, 63 (1), 24–40.

Lind P., Kjellström E., 2009, *Water budget in the Baltic Sea drainage basin: evolution of simulated fluxes in a regional climate model*, Boreal Environ Res., 14 (1), 56–67.

Ljungemyr P., Gustafsson N., Omstedt A., 1996, *Parameterization of lake thermodynamics in a high resolution weather forecasting model*, Tellus A, 48 (5), 608–621.

MacKenzie B. R., Gislason H., Möllmann C., Köster F. W., 2007, *Impact of 21st century climate change on the Baltic Sea fish community and fisheries*, Glob. Change Biol., 13 (7), 1348–1367

Meier H. E. M., 2006, *Baltic Sea climate in the late twenty-first century: a dynamical downscaling approach using two global models and two emission scenarios*, Clim. Dynam., 27 (1), 39–68.

Meier H. E. M., Andréasson J., Broman B., Graham L. P., Kjellström E., Persson G., Viehhauser M., 2006, *Climate change scenario simulations of wind, sea level, and river discharge in the Baltic Sea and Lake Mälaren region – a dynamical downscaling approach from global to local scales*, Rep. Meteorol. Climat. No. 109, SMHI, Norrköping, 52 pp.

Meier H. E. M., Döscher R., 2002, *Simulated water and heat cycles of the Baltic Sea using a 3D coupled atmosphere-ice-ocean model*, Boreal Environ. Res., 7 (4), 327–334.

Meier H. E. M., Döscher R., Faxén T., 2003, *A multiprocessor coupled ice-ocean model for the Baltic Sea: application to salt inflow*, J. Geophys. Res., 108 (C8), 3273, doi: 10.1029/2000JC000521.

Meier H. E. M., Eilola K., Almroth E., 2011, *Climate-related changes in marine ecosystems simulated with a three-dimensional coupled biogeochemical-physical model of the Baltic Sea*, Clim. Res., (in press).

Nakićenović N., Alcamo J., Davis G., de Vries B., Fenhann J., Gaffin S., Gregory K., Grübler A., Jung T. Y., Kram T., La Rovére E. L., Michaelis L., Mori S., Morita T., Pepper W., Pitcher H., Price L., Keywan R., Roehrl A., Rogner H.-H., Sankovski A., Schlesinger M., Shukla P., Smith S., Swart R., van Rooijen S., Victor N., Dadi Z., 2000, *Emission scenarios*, A Special Report of Working Group III of the Intergovernmental Panel on Climate Change, Cambridge Univ. Press, New York, N.Y., 599 pp.

Nordström M., 2006, *Estimation of gusty winds in RCA*, Uppsala Univ., M. Sc. thesis No. 101 (ISSN 1650-6553), 42 pp.

Omstedt A., Chen Y., Wesslander K., 2005, *A comparison between the ERA40 and the SMHI gridded meteorological databases as applied to Baltic Sea modelling*, Nord. Hydrol., 36 (4–5), 369–380.

Räisänen J., Hansson U., Ullerstig A., Döscher R., Graham L. P., Jones C., Meier H. E. M., Samuelsson P., Willén U., 2004, *European climate in the late 21st century: regional simulations with two driving global models and two forcing scenarios*, Clim. Dynam., 22 (1), 13–31.

Rockel, B. Woth K., 2007, *Extremes of near-surface wind speed over Europe and their future changes as estimated from an ensemble of RCM simulations*, Climatic Change, 81 (S1), 267–280.

Rubel F., Hantel M., 2001, *BALTEX 1/6-degree daily precipitation climatology*, Meteorol. Atmos. Phys., 77 (1–4), 155–166.

Samuelsson P., Gollvik S., Ullerstig A., 2006, *The land-surface scheme of the Rossby Centre Regional Atmospheric Climate Model (RCA3)*, Rep. Meteorol. No. 122, SMHI, Norrköping, 25 pp.

Samuelsson P., Jones C., Willén U., Ullerstig A., Gollvik S., Hansson U., Jansson C., Kjellström E., Nikulin G., Wyser K., 2011, *The Rossby Centre Regional Climate Model RCA3: model description and performance*, Tellus A, 63 (1), 4–23.

Savchuk O. P., Wulff F., 2007, *Modeling the Baltic Sea eutrophication in a decision support system*, AMBIO, 36 (2–3), 141–148.

Savchuk O. P., Wulff F., 2009, *Long-term modeling of large-scale nutrient cycles in the entire Baltic Sea*, Hydrobiologia, 629 (1), 209–224.

Solomon S., Qin D., Manning M., Chen Z., Marquis M., Averyt K. B., Tignor M., Miller H. L. (eds.), 2007, *Climate change 2007: the physical science basis*, Contribution of Working Group I to the Fourth Assessment Report of the Intergovernmental Panel on Climate Change, Cambridge Univ. Press, Cambridge, New York, N.Y., 847–940.

Udin I., Sahlberg J., Lundqvist J.-E., Uusitalo S., Seinä A., Leppäranta M., 1981, *BASIS: a data bank for Baltic sea ice and sea surface temperatures*, Res. Rep. No. 34, Winter Nav. Res. Board, Swedish Administration of Shipping Navigation and Finnish Board of Navigation, Norrköping, 23 pp.

Uppala S. M., Källberg P. W., Simmons A. J., Andrae U., Da Costa Bechtold V., Fiorino M., Gibson J. K., Haseler J., Hernandez A., Kelly G. A., Li X., Onogi K., Saarinen S., Sokka N., Allan R. P., Andersson E., Arpe K., Balmaseda M. A., Beljaars A. C. M., Van De Berg L., Bidlot J., Bormann N., Caires S., Chevallier F., Dethof A., Dragosavac M., Fisher M., Fuentes M., Hagemann S., Hólm E., Hoskins B. J., Isaksen L., Janssen P. A. E. M., Jenne R., Mcnally A. P., Mahfouf J.-F., Morcrette J.-J., Rayner N. A., Saunders R. W., Simon P., Ster A., Trenberth K. E., Untch A., Vasiljevic D., Viterbo P., Woollen J., 2005, *The ERA-40 re-analysis*, Q. J. Roy. Meteor. Soc., 131 (612), 2961–3012.

Wulff F., Bonsdorff E., Gren I.-M., Johansson S., Stigebrandt A., 2001, *Giving advice on cost effective measures for a cleaner Baltic Sea: a challenge for science*, AMBIO, 30 (4–5), 254–259.